# UV-fibers: two decades of improvement for new applications

Karl-Friedrich Klein[1,2], Valery K. Khalilov[3]

[1] Technische Hochschule Mittelhessen - University of Applied Sciences,
W.-Leuschner-Str. 13, D-61169 Friedberg (Germany)
email: Karl-Friedrich.Klein@iem.thm.de
[2] TransMIT GmbH, Saarstr. 23, 61169 Friedberg (Germany)
[3] Polymicro Technologies, 5th Avenue, Phoenix, Az (USA)

## ABSTRACT

Multimode UV-fibers with high-OH synthetic silica core and F-doped silica cladding have been available for over 40 years. At the beginning, the spectral UV-range above 250 nm wavelength was commonly used, because the generation of UV-absorbing defect centers prevented reliable light transfer below 250 nm; even light from a low-power broadband deuterium-lamp was sufficient to damage these UV-fibers of the 1st generation. However, even then, applications in the field of spectroscopy, laser light delivery, sensors and process control were discussed and improvements of fiber quality in this very interesting UVC range required by researchers and industrial end-users. Starting in 1993 with hydrogen-loaded fibers, further modification in preform and fiber manufacturing including additional fiber treatments lead to currently available hydrogen-free UV-fiber (4th generation) with significantly improved stability in the DUV-region below 250 nm, enabling routine use of optical fibers in this field. In addition to the UV-fiber improvements, some selected UV fiber-optic applications using broadband deuterium-lamps will be discussed. Finally, there is still room for further improvements, especially in combination with newly available pulsed UV light sources, which are low-cost, small sized and highly reliable.

**Keywords:** step-index fibers, multimode fibers, UV fibers, UV defects, UV fiber-optic systems, deuterium lamp, UV lasers, fiber-optic spectroscopy, chromatography

## 1. INTRODUCTION

The transmission of light from a light source to a sample and from this sample to a detector via specialty step-index (SI-) fibers is a standard fiber-optic method for medical and spectroscopic applications. Silica-based fibers with a high-OH undoped silica core and fluorine-doped cladding were selected for UV-applications because of lowest attenuation. Presented for the first time in 1974 /1/, these fibers have now been commonly used for over 40 years.

Around 1985, the interest in deep UV (DUV) applications started due to the introduction of new light-sources and spectral detector-systems. Unfortunately, some restrictions of the UV fibers in these fiber-optic systems became obvious: the life-time or time of operation in fiber-optic based systems were often limited by the generation of optically active defects in this wavelength region. Additionally, material and surface damages with pulsed lasers were observed at UV laser wavelengths. Over the past two decades, UV-properties, such as basic transmission and induced losses have been continuously improved in UV-fibers with a focus on deuterium-lamp usage. These improvements were achieved by preform modifications, novel fiber drawing techniques and fiber processing. Although high-OH fibers seemed most favorable, also low-OH fibers were optimized as wide range fibers for DUV and NIR region, from 200 nm up to 2200 nm wavelength. Details of these improvements leading to 4 generations of different fibers will be shown in following sections.

Parallel to improvements in UV fibers, testing equipment and testing methodology were developed and implemented to control quality and reproducibility of the various fiber generations. In addition to fluorescence analysis, several novel UV applications, such as fiber-optic thin-layer chromatography, liquid and gas spectroscopy and other analytical instrumentation will be shown in section 5, only to name a few. Some of these fiber-optic systems for analytical applications use light-sources with light power levels up to 10 mW.

## 2. STATUS OF UV-FIBERS ARROUND 1990

In 1990, silica was the most widely used material for the fabrication of light-guiding fibers in the region spectral between approximately 250 nm and 1.6 µm because of its low attenuation /2,3,4/. Unfortunately, the light transmission below 250 nm was not stable under certain conditions, which were often encountered in sensor systems, where, for example, the light source was a pulsed high-power laser /5,6,7/, an UV-laser /6,7/ or a deuterium lamp /8/. In the latter case, the wide potential spectroscopic applications were restricted to the wavelength region above 250 nm, because standard fibers were damaged by UV-light below 230 nm so quickly that a stable and acceptable transmission in any practical device was impossible.

In this section, a short overview about the properties of UV-fibers including their manufacturing is given, based on the knowledge at that time.

### 2.1 Optical properties of UV-fibers

For low-power transmission, only the UV basic attenuation (unit: dB/m) and the UV-induced loss (unit: dB) of a fiber with defined length have to be taken into account. Using (pulsed) laser, the total transmission is additionally reduced by two photon-absorption.

### 2.1.1 Basic attenuation

In the spectral region at $\lambda < 400$ nm wavelength, the basic attenuation, $\alpha_B(\lambda)$ in undoped silica or silica fibers with an undoped core, essentially depends on UV-intrinsic losses and on Rayleigh scattering /2,3,4/. Using the standard cut-back method /9/, the difference length $\Delta L$ has to be adjusted to the increasing attenuation values and the decreasing dynamic of the measurement system with decreasing wavelength $\lambda$. A typical result is shown in Fig. 1.
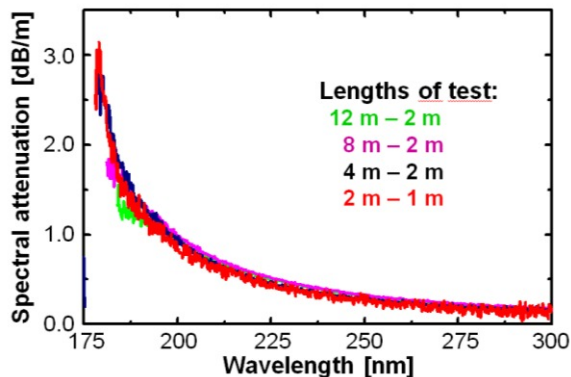


Fig. 1: Basic attenuation of a 600 µm core SI fiber due to Rayleigh scattering and electronic transitions; the cut-back method was used with different lengths to overcome the dynamic restrictions of the test system
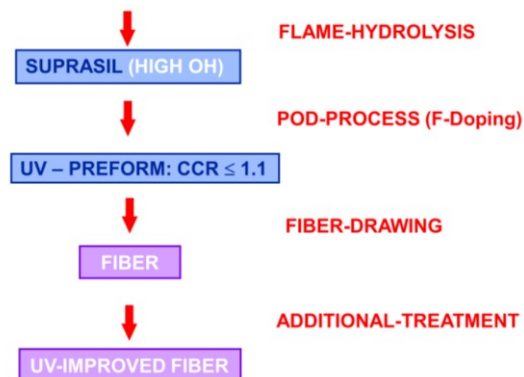


Fig. 2: Manufacturing steps of UV-fiber with high-OH silica core /1,2,10-12/

### 2.1.2 UV-defects – an overview

Optically active defects in silica or silica fibers can be generated by low-power broadband deuterium-lamps and pulsed excimer-lasers, as summarized in Table 1. Especially the E'-center ($\equiv$Si$^{\bullet}$: silicon with one unpaired electron) with an absorption band at 214 nm and the Non-Bridging-Oxygen-Hole center NBOHC ($\equiv$Si-OH°) at 260 nm are well known in high-OH silica. In addition, Oxygen-Deficient-Centers (ODCs) around 250 nm are observed in low-OH silica. In more detail, overviews on UV-defects can be found in /2,6-8,13-19/.

The concentration of each defect is dependent on several factors, including preform contaminants, preform manufacturing technique and fiber draw process including fiber post-treatments.

**Table 1:** Overview about relevant defects and impurities in high OH fibers /13-19/

| Defect Description | Chemical Structure | Comment |
|---|---|---|
| E'-center | $\equiv Si^{\bullet}$ | Absorption band at 214nm |
| Non Bridging Oxygen Hole Center (NBOHC) | $\equiv Si\text{ - }O°$ | Absorption bands at 260nm and 620nm |
| Silicon without unpaired electron | $\equiv Si^{+}$ | Absorption band at 163nm |
| Strained Silica bond | $\equiv Si - O\text{ - }Si \equiv$ | Weakened regular bonds |
| Chlorine impurity | Cl - Cl | Absorption band at 320nm |
| HCl impurity | H - Cl | Absorption band near 165nm |
| SiH impurities | Si – H | Precursor |

### 2.1.3 UV-induced losses

Measuring UV-induced losses, $\Delta a_L(\lambda)$ (unit: dB), the wavelength- and position(z)-dependencies of the UV-induced attenuation, $\Delta\alpha(\lambda,z)$, play a significant role. With a low-power broadband DUV light-source, the light-guiding core material will be damaged by generating E'-centers and/or NBOHCs (see Table 1) by UV-photons with energy hν:

$$\equiv Si\text{ - }0\text{ - }Si \equiv \ + h\nu \ \rightarrow \ \equiv Si \bullet \quad \bullet 0\text{ - }Si \equiv \tag{1a},$$

$$\equiv Si\text{ - }Cl \qquad + h\nu \ \rightarrow \ \equiv Si \bullet \quad \bullet Cl \tag{1b}.$$

In a fiber with a defined length, L, the extent of defect generation decreases along the fiber with position z due to the fact that the fiber behaves as a long pass filter. Therefore, the induced loss, $\Delta a_L(\lambda)$, does not increase linearly with the length of the fiber:

$$\Delta a_L(\lambda) = \int_0^L \Delta\alpha(\lambda,z)dz \tag{2}.$$

In addition, the damage is time-dependent, leading to the following equation for the total loss $a_{L,tot}$ with a well-defined fiber length, L, where $t_{UV}$ is the UV-exposure time:

$$a_{L,tot}(\lambda, t_{UV}) = \alpha_B(\lambda) L + \Delta a_L(\lambda, t_{UV}) \tag{3}.$$

### 2.2 Fiber manufacturing

The above mentioned UV fibers are manufactured in several steps, as shown in Fig. 2. A rod of high-OH synthetic silica is produced by flame-hydrolysis /10,12/ using silicon tetrachloride in an oxygen-hydrogen burner. With Plasma Outside deposition (POD) this rod is cladded with silica having a fluorine content of approx. 3%. The obtained UV-preform has a Cladding-Core-Ratio, CCR, typically in the order of 1.1 or smaller /2,10/. Such performs with diameters > 15 mm are drawn into so-called All-Silica-(AS-)fibers, with core diameters between 50 to 1000 μm. To improve UV optical performance, additional preform and fiber treatments can be carried out.

### 2.3 Fiber testing

In Fig. 3, a principle setup for testing the UV damage of fibers during UV irradiation with a deuterium lamp is shown; this setup was used for confirming the transmission improvements in R&D and for quality control in production. All spectral measurements were performed using a standard deuterium ($D_2$) lamp DO660/05J from Heraeus Noblelight /20/ as a broadband light source and an optimized imaging system. The distal end of the Fiber under Test, FUT, is coupled into a fiber-optic spectrometer (FOS) USB4000 from Ocean Optics /21/ with an UV-enhanced grating for deep-UV used as detector system, DS.

In order to reduce the noise in the FOS-signal and in the UV-induced loss spectra, either an adjacent average with 9 points or a Fast-Fourier-Transformation smoothing filter with cut-off frequency of 0.36 (arb. units) using 15 supporting points were employed. The entire system for measuring the spectral UV-induced losses at room temperature is described in details elsewhere /22-24/.

Optionally, a gas-tight box, which can be purged with inert gases, e.g. nitrogen, to avoid oxygen absorption below 195 nm, was used. The position of the shutter, Sh, is controlled by software via an electrical TTL output of a computer. Two cases are distinguished. With an open shutter, the photo-darkening of the FuT with the $D_2$ lamp is measured. During recovery after UV damage, the deuterium irradiation is blocked to avoid additional damage. For each measurement point, however, the shutter is opened for 2 … 5 s, only; within this short period in comparison to the long period of darkness, the UV damage is negligible /22-24/.
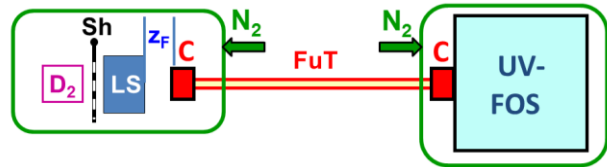


*Fig. 3: Measurement setup for damaging the UV-fibers with the following components: D2: deuterium lamp; LS: lens system; C. SMA-connector; FuT: fiber under test; UV-FOS: fiber-optic spectrometer with deep UV detection; $z_F$: axial distance between lens system and fiber front face; $N_2$: nitrogen purge, when required*

The FOS signal, FOSS($\lambda$,t), is proportional to the spectral power densities, at a given wavelength. However, the transfer factor from input power or density to photo current or charge is strongly wavelength dependent. The spectral and temporal UV-induced losses (unit: dB) can be determined as follows:

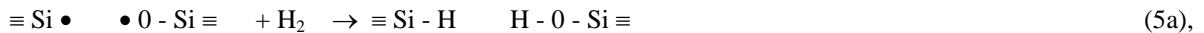$$\Delta a_L (\lambda, t_{UV}) = 10 * \log (FOSS (\lambda, t_{UV}=0) / FOSS(\lambda, t_{UV})) \tag{4}.$$

Either, the spectral losses $\Delta a_L(\lambda, t_i)$ at given times $t_i$ or the temporal losses $\Delta a_L(\lambda_n, t_{UV})$ at given wavelengths $\lambda_n$ are determined.

## 3. UV FIBER IMPROVEMENTS

### 3.1 UV fibers with high-OH silica core

In 1993, standard UV fibers (type: FVP /11/; 1st generation) drawn from standard UV preforms /10/ had a very low basic attenuation, with values of < 1.0 dB/m at 200 nm (see Fig. 1). However, these fibers were darkened below 230 nm during UV irradiation with deuterium lamps within 11 h (Fig. 4); the UV induced losses at 214 nm of such 1 m long fibers were between 10 to 40 dB, depending on different manufacturing and testing parameters (Fig. 5). In addition to the high values, the recovery of the fiber was an issue, too: the concentration of transient E'-centers was decreasing with time constants of several hours.

The stimulating step was the hydrogen-loading of the standard UV fibers (type: UVI; 2nd generation), described in /25/ for the first time. The E'-centers generated by UV-light (see eq. 1) were passivated as follows:

$$\equiv Si \bullet \quad \bullet 0 - Si \equiv \quad + H_2 \quad \rightarrow \equiv Si - H \quad H - 0 - Si \equiv \tag{5a},$$
$$\equiv Si \bullet \quad \bullet Cl \quad + H_2 \quad \rightarrow \equiv Si - H \quad H - Cl \tag{5b}.$$

Comparing with Fig. 4, these fibers exhibit no UV-induced losses within 11 h of UV-irradiation (Fig. 6). Testing three different fiber samples, the same behavior was confirmed for 11 hours (Fig. 7). Only small differences were observed in the short-term behavior because the precursor and defect concentrations could have been different due to processing of preform and fiber. In addition, similar improvements were found with KrF-laser irradiations (Fig. 8).

This first step of improvement enabled several new applications where DUV light was required. However, for many applications using small fiber diameters the predicted life-time due to hydrogen out-gassing was not sufficient /26-29/.

Because of an increased demands for non-loaded fibers, the preform manufacturing process was modified and a new product was announced in 1999 /30,31/. Using this modified preform without any significant changes in the drawing process, the 3rd generation of UV fiber became commercially available /10,11/. However, transient defects were still too high leading to signal drifts and uncertainties in the application set-ups.

Finally, additional changes in fiber-drawing and post-treatments lead to a further improved fiber (4th generation) with lowest permanent and transient defect concentrations /32/, using the proposed 4 h test described in section 2.3.

Over several design generations, the UV damage at 214 nm wavelength of high-OH fibers has been reduced significantly. These steps and the increased UV-stability are shown in Fig. 9 and Table 2.

Focusing on the two main defect centers, Fig. 10 shows the temporal damage of a commercially available FDP-fiber (4th generation) with 100 µm core diameter. In the proposed 4 h test (section 2.3), the UV-induced loss at 214 or 266 nm loss in a 2 m fiber sample will be below 0.8 dB or 0.3 dB, respectively. Starting with the FVP-fiber (1st generation), the normalized transmission at 214 nm wavelength increased from 0.1 % to > 90 % for the FDP-fiber. However, a longer UV test of 48 hours was carried out leading to an additional increase of 214 nm absorption band after a first saturation (around 4 hours), as shown in Fig. 11 /33/. For 260 nm band, on the other hand, it is obvious that no saturation can be observed. After 48 hours, both absorption bands seemed to have the same value due to different rates of increases:
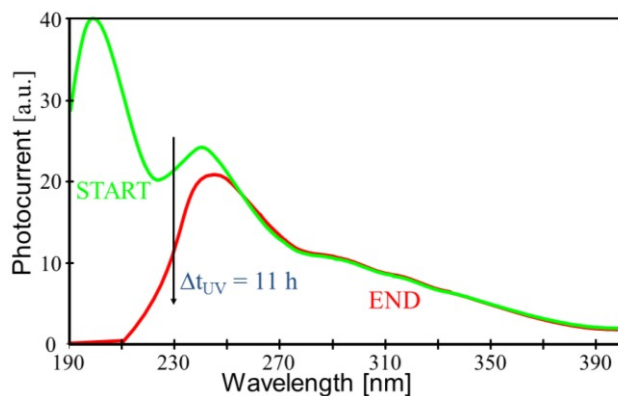


*Fig. 4:* *Wavelength-dependent transmission, expressed by photocurrent, before and after 11 h of UV-irradiation of a 1.0 m long UV-fiber of 1st generation; the darkening below 230 nm is due to the generation of E'-centers /25/*
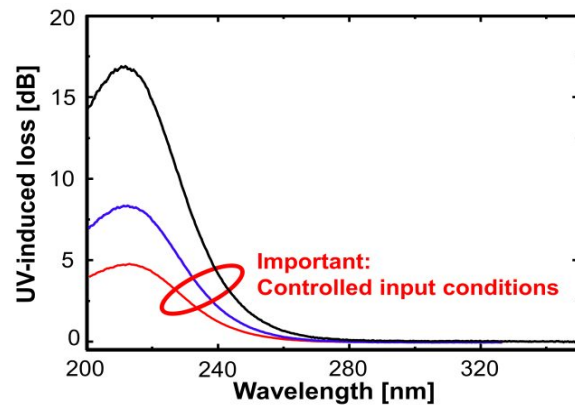


*Fig. 5:* *Saturated UV-induced loss after (only) 4 h of UV-irradiation, using UV-fibers from the same draw and a stronger deuterium-lamp; the different graphs are generated with different input conditions /8,24/*
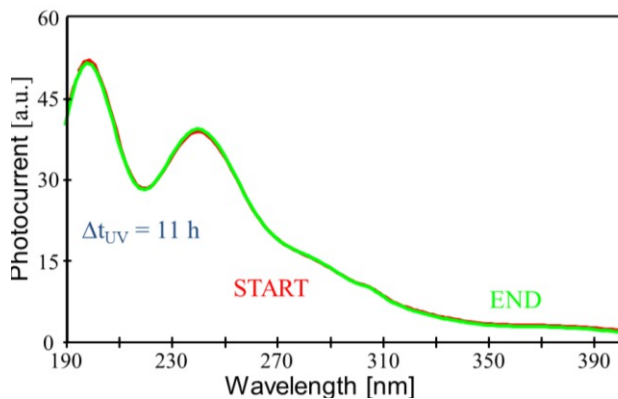


*Fig. 6:* *Wavelength-dependent transmission, expressed by photocurrent, before and after 11 h of UV-irradiation of a 1.0 m long UV-fiber of 2nd generation; the darkening below 230 nm is avoided due to hydrogen-content in the light-guiding core /25/*
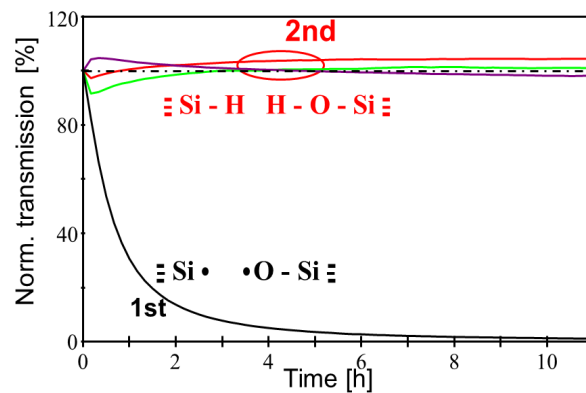


*Fig. 7:* *Comparison of the UV-damages of 1.0m long UV-fibers from 1st generation (1 piece) and 2nd generation (three samples) using deuterium-lamp, described by the temporal transmission at 214 nm wavelength (maximum of E'-center absorption) for 1.0 m long UV-fibers; the defects generated by UV-light and the passivation with hydrogen is indicated /25/*
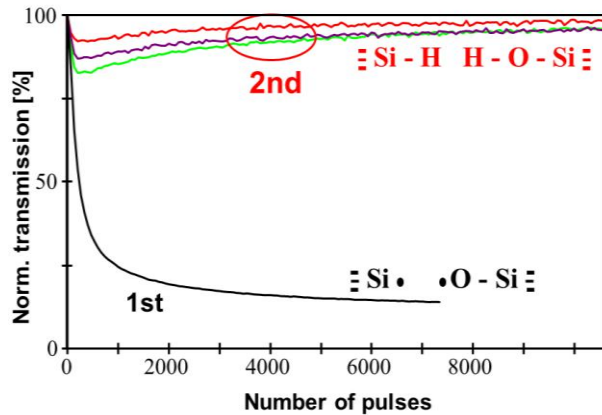
Fig. 8: like Fig. 7, however the fiber is damaged by a KrF-laser (248 nm) and transmission is monitored at 248 nm, too /25/
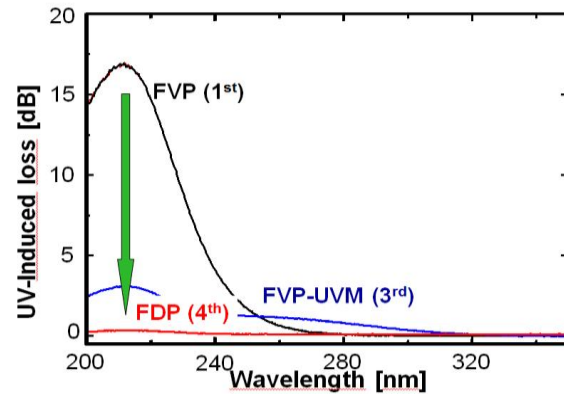
Fig. 9: Comparison of the different hydrogen-free fibers in respect to the spectral UV-induced loss after UV-irradiation of 4 hours (saturation); the fiber lengths are different: 1 m for FVP, 2 m for FVP-UVM and FDP

**Table 2:** History of different high-OH fibers with reduction of UV-induced losses at 214 nm

| Generation | Fiber/ preform type | UV-induced loss at 214 nm in 2 m long fibers | Comments |
|---|---|---|---|
| | | | |
| 1 | FVP [11]/ Standard [10] | 20 … 40 dB | |
| 2 | UVI | < 1 dB | Hydrogen loaded fibers, with defect passivation; diameter-dependent out gassing leads to FVP fiber |
| 3 | FVP-UVM [11]/ SBU [10] | < 6.5 dB | Hydrogen-free fiber; improvement due to preform modifications /29/ |
| 4 | FDP [11] | < 1.0 dB for 200 … 600 μm core | Hydrogen-free fiber; improvements due to preform and fiber modifications /30,31/ |
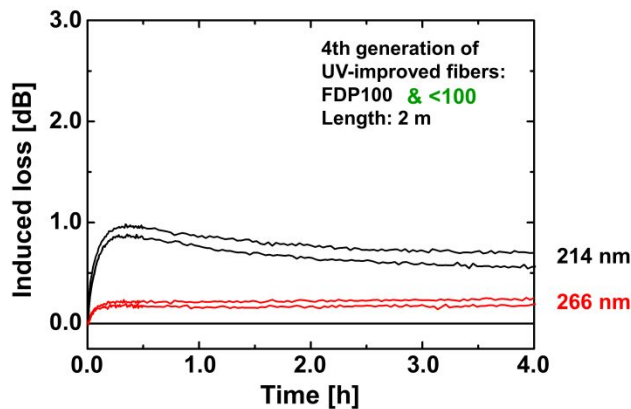




Fig. 10: Temporal UV-induced loss of 2 m long FDP-fibers (4th generation) samples having <90 μm and 100 μm core diameter, shown for 214 nm (E'-center) and 266 nm (NBOHC)
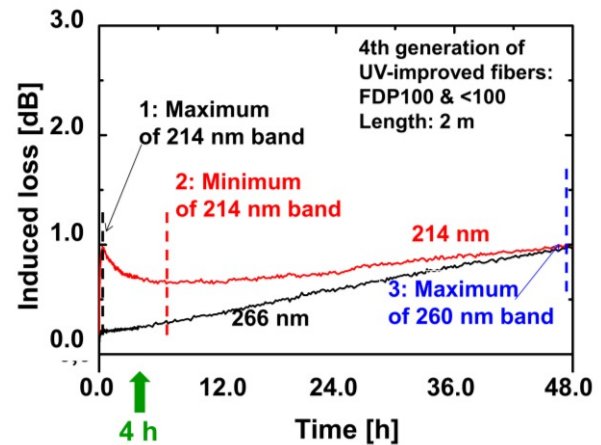
Fig. 11: Long-term fiber damage with UV-light using a deuterium-lamp like in the 4 h test /33/

Further improvements lead to the newest results, shown in Fig. 12. Now, both absorption bands are nearly constant for at least 72 hours or 3 days of continuous UV-irradiation with a deuterium-lamp. These newest results were published in /34,35/. In addition, the optical UV properties can be determined leading to a certified UV-fiber /11,36/, using the described measurement set-up above.
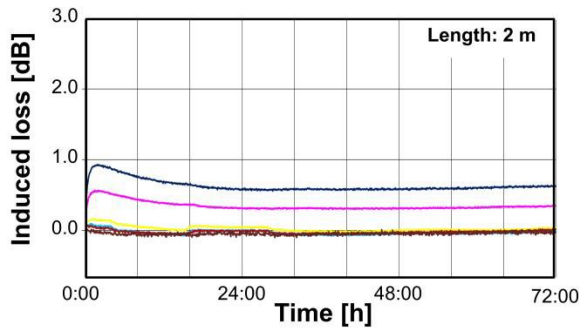
Fig. 12: Long-term over 72 hours for a further improved FDP-fiber with 100 μm core diameter /35/

### 3.2 UV fibers with low-OH silica core

On first view /37/, high-OH fibers seemed to be favorite for DUV applications. As seen in Fig.13, the basic attenuation is very high, especially around 214 and 250 nm. These drops in transmission are related to the well-known E'-centers and Oxygen Deficient Centers (ODC) in low-OH material.

Similar to the improvement from 1st to 2nd generation of high-OH, hydrogen loading will increase the basic UV transmission per meter or reduce the basic UV attenuation significantly (Fig. 14). The gain in attenuation for this selected sample of a low-OH fiber with 600 μm core diameter was: > 10.0 dB/m at 214 nm and > 5.0 dB/m at 250 nm (Fig. 15).
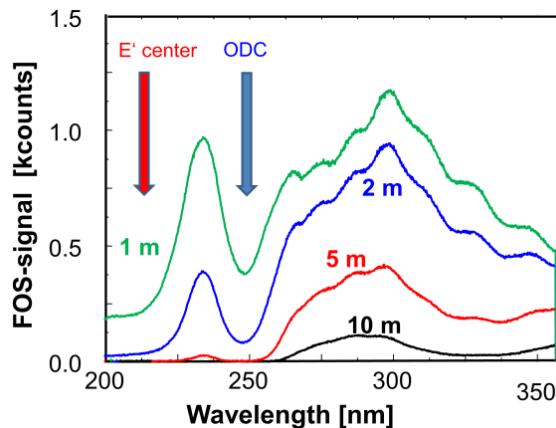


Fig. 13: Spectral transmission due to basic attenuation in low-OH SI-fibers with 200 μm core diameter; E'-centers at 214 nm and Oxygen Deficient Centers (ODC) at 250 nm are dominant /37/
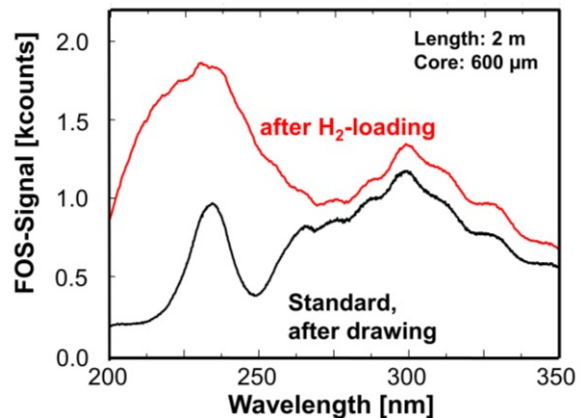


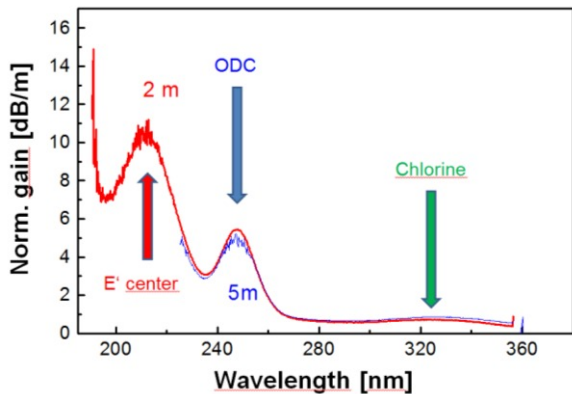Fig. 14: Enhanced UV-transmission of low-OH SI-fibers after hydrogen-loading /37/



Fig. 15: Spectral gain, normalized to 1.0 m, using the graphs in Fig. 12 /37/
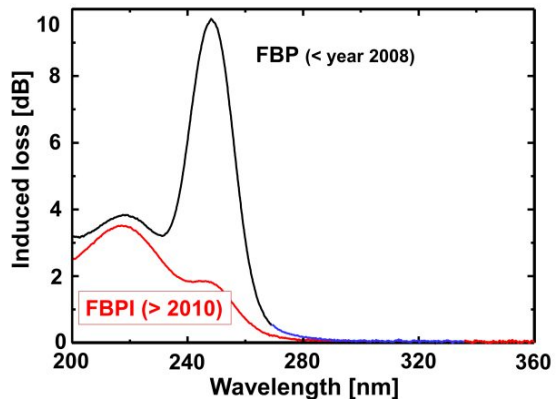


Fig. 16: Spectral UV-damage of broadband low-OH fiber after 4 h UV-irradiation with deuterium-lamp /38/

A slight decrease in attenuation at 330 nm due to chlorine modifications is obvious, too. The overall output power in dependence of the wavelength or the spectral attenuation is very similar for low-OH and high-OH fibers. As discussed in /37/, however, the starting performance of the low-OH fiber has a strong influence on the final one, after hydrogen loading. In some cases, the ODCs could not be suppressed totally.

Further processing steps have been added leading to a hydrogen-free low-OH fiber with excellent IR-performance and excellent UV-stability (Fig. 16). The final product FBPI /11,38/ is used in several new applications, e.g. in astronomy.

## 4. NEW UV LIGHT-SOURCES AND FIBER-DAMAGE

The damage of UV-fibers has mainly been studied with broadband low-power deuterium-lamps and pulsed excimer-lasers. In the last 5 years, however, new and reasonably priced UV light-sources with interesting features became commercially available:

- Broadband Laser-driven light-source LDLS /39/
- UV-LEDs /40,41/
- Pulsed UV-lasers based on higher harmonics Nd-YAG lasers /42/.

In Fig. 17, the (relative) spectral output power out of a 100 µm core is shown using three UV light sources under test and a deuterium-lamp as a reference /33,43/. As shown, the power levels are significantly higher compared to the deuterium lamp: especially, the integration time for the deuterium-lamp was at least 2 magnitudes of order higher.

The surprising results for the laser-driven plasma lamp LDLS are shown in Fig. 18 & 19 /33/. After a sharp increase of the typical absorption bands at 214 and 265 nm, the maximum of 1.75 dB is reached after approx. 1 min. Although the spectral power in the fiber was at least 20 dB higher, significant annealing took place leading to a saturation level of 0.7 dB due to photo-bleaching with strong IR-light /44/; with the same fiber, the saturated induced loss at 214 nm was 2.5 dB using the standard set-up with deuterium-lamp as a reference. Focusing on 265 nm, no saturation is obvious after 4.0 hours of LDLS irradiation.

Using pulsed 3$^{rd}$ harmonic Nd-YAG-laser /33/ with very high pulse power, the UV-induced damages are significantly higher (Fig. 20), in comparison to the deuterium lamp after 4 hours. With increasing pulse energies, the 260 nm absorption (NBOHC, see table 1) is growing stronger indicating that additional effects appear. In order to understand these effects more clearly, further tests are planned.
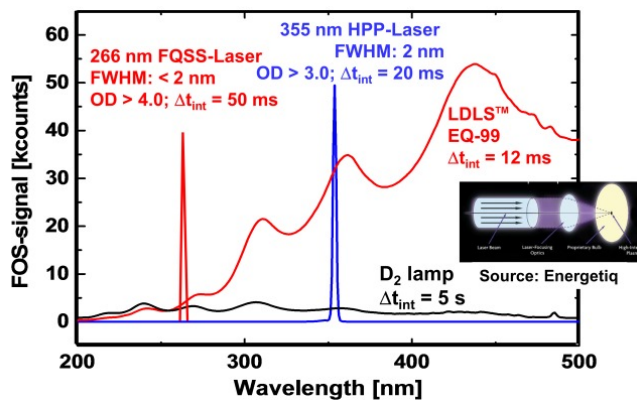


Fig. 17: *The spectral output power of new commercially available UV Light-sources, measured with a 100 µm core fiber; in addition to two pulsed Nd-YAG-lasers with 266 and 355 nm wavelength /33,42,43/, a Laser-driven broadband (plasma) lightsource (LDLS, /39/) has been used, which is continuously (cw) irradiating*
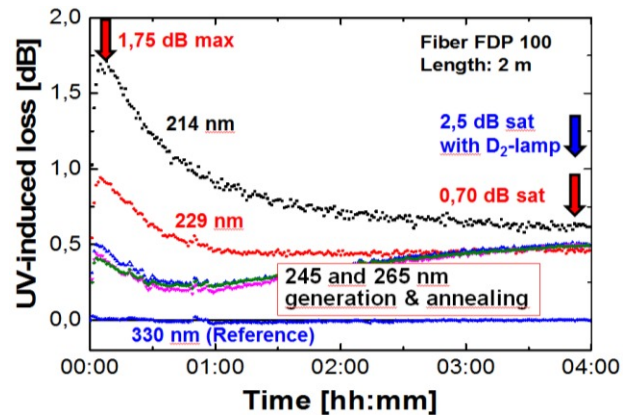
Fig. 18: *Temporal UV-induced loss of 2 m long FDP-fibers (4$^{th}$ generation) samples having 100 µm core diameter, using the new LDLS /39/; similar data after 4 h tests with deuterium-lamp is included in the figure; the absorption around 250 and 266 nm is not in saturation, after 4 h tests*
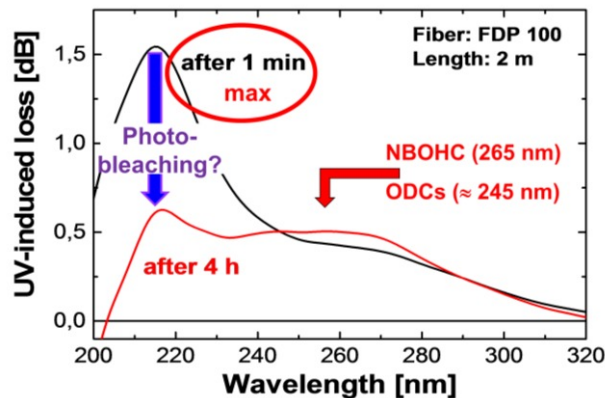
*Fig. 19:* Spectral UV-induced loss of 2 m long FDP-fiber (4th generation) samples having 100 μm core diameter, using the new LDLS /39/; a strong local maximum at 214 nm is shown within less than 5 minutes followed by a reduction at 214 nm and an increase at 265 nm after 4 h UV-irradiation with new plasma-lamp
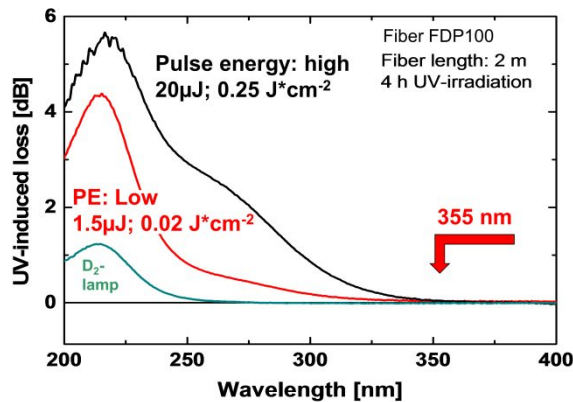
*Fig. 20:* UV-damage of FDP100 fiber due to pulsed 3rd harmonic Nd-YAG laser light in comparison to a 4h test using standard deuterium-lamp; two different lasers have been used /33,42,43/

## 5. FIBER-OPTIC APPLICATIONS IN UV REGION

As indicated before, UV-applications have been stimulated by further improvements of UV-fibers. Although the hydrogen-loaded UV-fibers of the second generation are not widely used, especially for small diameters, these fibers were door-openers for new fiber-optic UV applications, as follows:

- Cross-section converters /11,21,45-47/
- Diode-array (DA) Thin-Layer-Chromatography (TLC) /46-48/
- Fiber-optic HPLC /49,50/
- Liquid-core waveguides and flow cells /49,51/
- UV-Gas analyses with Hollow-Core Waveguide (HCW) /52-54/
- Laser-induced fluorescence (LiF) /55,56/
- UV laser scalpel /57/
- UV-RAMAN /58-61/
- Cryogenic temperature application /62-64/
- Process control /65/.

### 5.1 Liquid-Core-Waveguides and flow cells

Some time ago, Liquid-Core-Waveguides (LCW) and flow cells (FC) for UV applications were studied in detail. Using Teflon on the outer side of a silica capillary, a light-guiding waveguide can be built up with all liquids in the capillary bore as long as the refractive index is higher than that one of Teflon /49,66/. In Fig. 21 an optical fiber based flow cell is shown /51/. Using the well-known Lambert-Beer's law, the effective path length in the LCWs or FC is smaller than the distance (physical path length) between the two optical fibers due to the partial propagation of light in the non-absorbing silica tube (see $l_{cap}$ in Fig. 21). This issue was discussed in detail in several papers (see /51/).

Some examples of spectral absorption measurements are given, for acetone (Fig. 22) and toluene (Fig. 24) with different concentrations in pure water. As expected, the absorption of acetone at the maximum absorption at 266 nm is linearly increasing with the concentrations, in the range from 20 mg/l to 300 mg/l (Fig. 23). Above that level, saturation is obvious caused by the dynamic range of the measurement set-up.
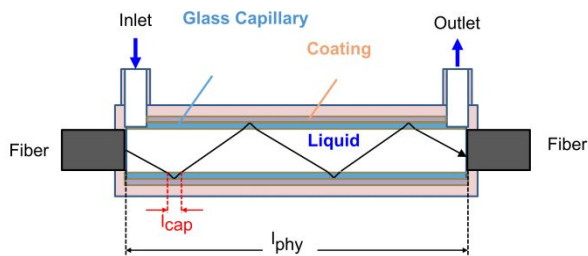
Fig. 21: *Sketch of a fiber-coupled Liquid-Core-Wave-guide (LCW) or flow cell; due to total reflection at the Teflon-coating, some portion of the light is propagating in the non-absorbing silica capillary /49,51/*
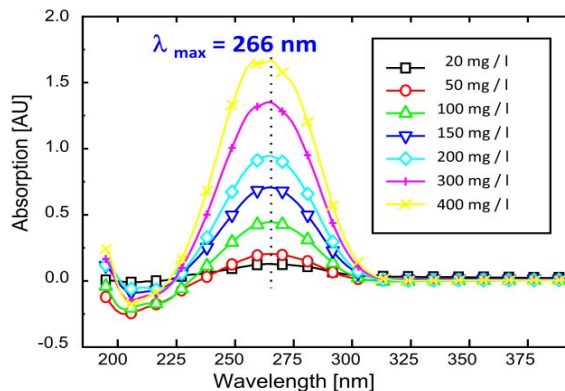


Fig. 22: *UV absorption spectra of acetone in water, for different concentrations /66/*
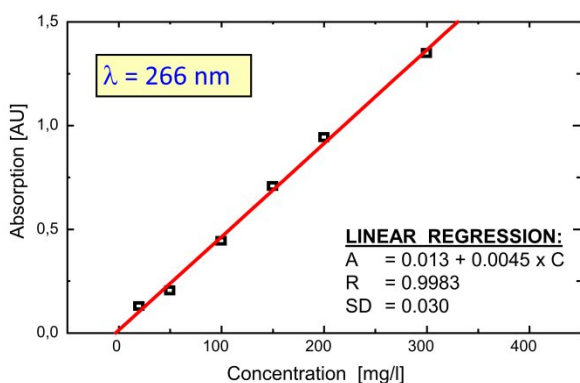


Fig. 23: *Concentration-dependent absorption of acetone in water at 266 nm (absorption maximum), based on the raw data in Fig. 20 /66/*
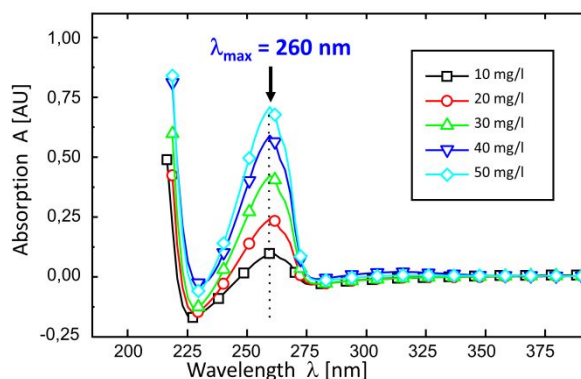


Fig. 24: *UV absorption spectra of toluene in water, for different concentrations /66/*

## 5.2    Hollow-Core-Waveguides for gas analyses

With a similar set-up, gas absorption can be measured in the UV-region (Fig. 25). Using short-length fibers, the possible wavelength region can reach 185 nm and below easily; however, the dynamic range is decreasing with decreasing wavelength, mainly caused by stray light effects in the polychromatic detector and in the application.

As shown in Fig. 24, the different gases have specific structures in their absorption spectra: the UV "finger-print" of the gas under test. Only ethanol has a non-specific spectrum with only broad absorption band. More details are in /52-54/.

## 5.3 Diode-array (DA) Thin-Layer-Chromatography (TLC)

The last example of our selection is the spectral Thin-Layer-Chromatography in the UV-region with diode-array which can only be realized with fiber-optic bundles /45-47/.The separation technique itself including the preparation will not be explained in this paper; details are in /48/.

In Fig. 27, the principle set-up for spectral TLC with fiber-optics is shown: without any analyte (a) on the plate the light from the "emission fiber" will be reflect and/or re-emitted from the surface layer and collected by the "detection fiber". The numerical aperture and the distance to the plate are the key parameters for the light coupled between the two fibers /46,47/. With analytes (b), the measured spectrum will be changed by the spectral absorption losses in the analytes. For the first time on a TLC-plate, fluorescence can be used for analyses, too. In mode A (c), the fluorescence of the analyte will be collected directly by the "detector fiber". However, having a fluorescent layer on the plate, this emission light can be modulated by the analyte due to absorption, as seen in mode B (d).

In Fig. 28, the difference spectrum (in dB) of an absorbing and fluorescent analyte is shown. For positive sign, the light is attenuated due to absorption; for negative sign, the measured signal is higher due to additional fluorescence. As an example, spectral TLC with fiber-optics is capable to distinguish between 16 Polycyclic Aromatic Hydrocarbon (PAHs);

using absorption and fluorescence. In addition, the positions of the separation are different (Fig. 29). While only one PAH can be detected easily by fluorescence, 5 PAHs will be optically separated using absorption spectra only.
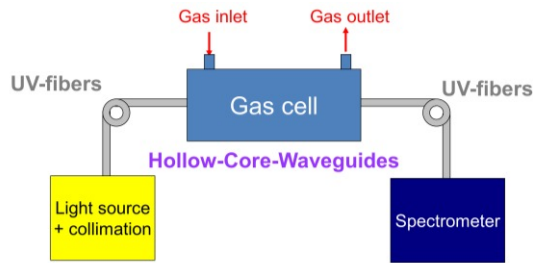


Fig. 25: Overview about fiber-coupled set-up for measuring gas absorption with long-length Hollow-Core-Waveguides (HCW, /67/) in the UV-region
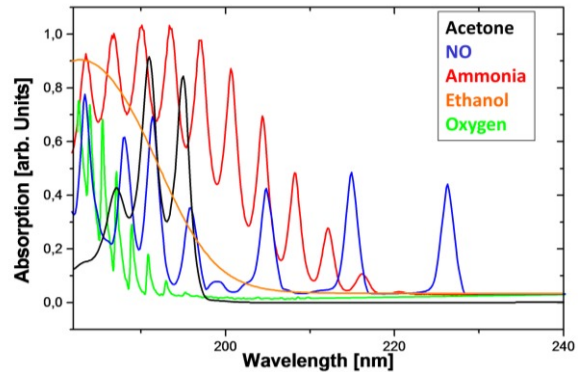


Fig. 26: Examples of absorption spectra of acetone, nitric oxide, ammonia, ethanol and oxygen, measured in a 1 m long HCW /52-54/
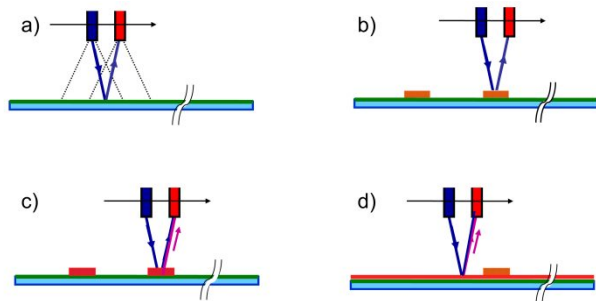


Fig. 27: Fiber-optic Thin-Layer-Chromatography; principle light-path and emission and acceptance cones of moving fibers (a), absorption mode with absorbing analyte on the plate (b), fluorescence mode A with fluorescent analyte (c) and fluorescence mode B with additional fluorescent layer on the plate plus an absorbing analyte (d)
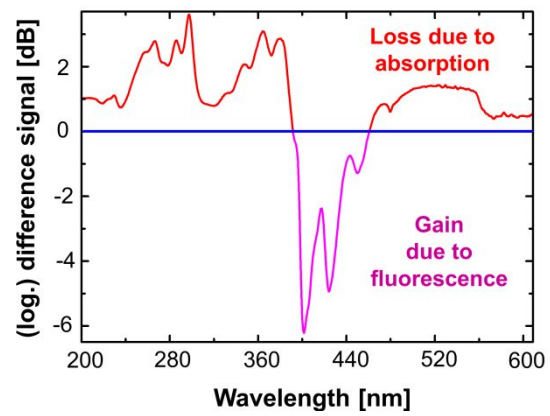


Fig. 28: Difference spectrum of an absorbing and fluorescent analyte on the TLC-plate /46/
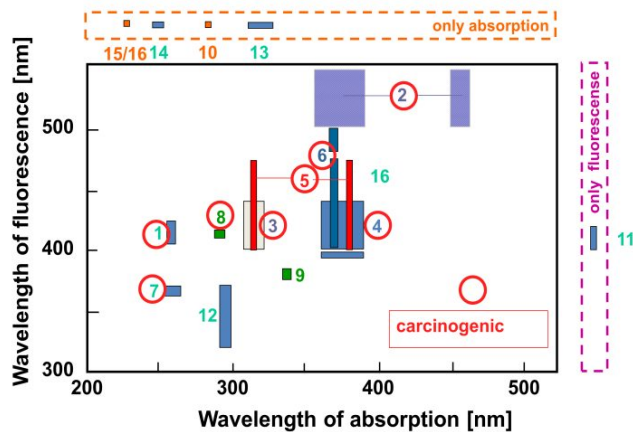


Fig. 29: Spectral results with 16 PAHs, having only absorption, only fluorescence or a combination of both /46,47/

# 6. SUMMARY AND OUTLOOK

UV-damages in silica based UV-fibers have been significantly reduced over the last two decades. Although no solarization-free material has been found so far, the achieved induced losses of < 0.6 dB at 214 nm and < 0.3 dB at 265 nm for 2 m long hydrogen-free fibers with 200 μm core are very impressive. Transient defects, mainly problematic in applications, such as e.g. UV-VIS HPLC detectors, where constant light delivery in the 200 to 250 nm is essential for baseline stability, are extremely low. In addition, the basic attenuation below 200 nm can be guaranteed. As a result, certified UV-fibers including both parameters are commercially available.

It is obvious that the relevant measurement techniques were required to detect and prove these improvements. In a first step, a system to measure UV attenuation at 190 nm wavelength and below was designed, using the cut-back method. However, the most important innovation was a measurement system for spectral and temporal UV-damage, where UV damages were split into permanent and transient components. It turned out that a low-power broadband deuterium-lamp was an excellent light-source for these requirements. However, the coupling conditions of the light beam into the fiber had to be optimized to get highest UV-damage levels. The next step will be the standardization of this measurement technique for optical degradation of UV-fibers. Taking the above mentioned results (section 2.3) into account, a first draft will be proposed by the German Institute for Standardization (DIN) "Fiber optics" within this year.

A multitude of fiber-optic UV applications have been mentioned. Based on novel UV light-sources, new UV applications were and will be stimulated. A small selection of these for us very interesting applications has been described in more detail above. These applications appear to have the potential for a commercial success in the near future, although they have been studied in R&D for more than one decade.

The temporal and spectral behavior of UV-light induced defects in silica was found to be very different, using high-power broadband plasma source, LDLS, or pulsed UV-lasers. On one side, significant annealing in addition to defect generation was observed, due to NIR-light of such LDLS. Future work will concentrate on the photobleaching effect, varying the spectral power above 400 nm in the fiber. On the other hand, UV-damage at 214 nm & 260 nm including a tail into the longer wavelength region was found to be significantly higher with UV-lasers than with low power deuterium lamp sources. As these effects are not totally understood, further experimental data will be collected with such lasers, in the near future.

After more than two decades, there are still open questions about the damaging mechanism of UV light in UV-fibers with undoped silica core and F-doped cladding. As an outlook, current and future applications will generate a multitude of new R&D-projects to study and further improve the properties of fibers and fiber-optic systems.

# 7. ACKNOWLEDGEMENT

# 8. REFERENCES

/1/ K.Rau, A.Mühlich, N.Treber: "Progress in silica fibers with fluorine dopant". Proc. OFC 1977, paper TuC4 (Williamsburg, 1977)

/2/ K.-F.Klein,A.Mühlich: "Quarzglas für unterschiedliche Anwendungen im Bereich von 0.2 µm und 2.4 µm (in German)". VDI-Berichte 673, p.147-177. (Karlsruhe, March 1988)

/3/ W.Heitmann: Attenuation analysis of silica-based single-mode fibres", J. Opt. Comun. 11, (1990), pp.122-124

/4/ G.H.Sigel jr.: "UV spectra in silicate glasses". J.-Non-Cryst.Solids, Vol. 13, pp. 372-398 (1973/74)

/5/ R. H. Stolen, Non-linear properties of optical fibres", in Optical Fiber Communications, Acad. Press, New York (1979), pp. 125ff

/6/ K.-F.Klein,G.Hillrichs,P.Karlitschek,K.Mann: "Possibilities and limits of optical fibers for the transmission of excimer laser radiation". SPIE-Proc. Vol.2966 „Annual Boulder Damage Symposium", S.564-573 (Boulder, Oct. 1996)

/7/ P. Karlitschek, G. Hillrichs, K.-F. Klein: "Photodegradation and nonlinear effects in optical fibres introduced by pulsed UV-laser radiation", Opt. Comm. 116, (1995), 219.

/8/ H. Fabian, U. Grzesik, K.H. Worner and K.-F. Klein: "Optical fibre for UV-applications", Proc. SPIE 1513

/9/ D. Marcuse: "Principles of Optical Fiber Measurements", Academic Press Inc., New York 1981, ISBN-13: 978-0124709805

/10/ Heraeus Quarzglas, Hanau (Germany): Brochures about Suprasil™ and Fluosil™ (www.heraeus.com)

/11/ Polymicro Technologies, Phoenix (USA): Data sheets about All-Silica Fibers (www.polymicro.com)

/12/ T. Li, Optical fiber communications: Volume 1 Fiber Fabrication, Academic Press (1985)

/13/ D.L.Griscom: „Defect structures of glasses". J.Non-Cryst. Solids. Vol. 73, pp. 51-78 (1985)

/14/ E.J.Friebele, D.L.Griscom: "Radiation effects in glass" in "Treatise on material science and technology". Acad.Press, New York, pp. 257-351 (1979)

/15/ E.J.Friebele, et.al.: "Overview about Radiation Effects in Fiber Optics". SPIE-proc. 541, pp. 70 (1985)

/16/ R.A.Weeks: "The many varieties of E'-centers: a review". J.-Non-Cryst.Solids, Vol. 179, pp. 1-9 (1994)

/17/ L.Skuja: "Optically active oxygen-deficiency-related centers in amorphous silicon dioxide". J.-Non-Cryst.Solids, Vol. 239, pp. 16-48 (1998)

/18/ V.Kh.Khalilov, G.A.Dorfman, E.B.Danilov, M.I.Guskov, V.E.Ermakov: "Character, mechanism of formation and transformation point defects in type IV silica glass". J.-Non-Cryst.Solids, Vol. 169, pp. 15-28 (1994)

/19/ R.West: "Radiation effects on fibre optics". SPIE-Proc. Vol. 867, pp. 2-9 (Nov. 1987, Cannes, France)

/20/ Heraeus Noblelight, Hanau (Germany): Brochure about standard deuterium lamps and Fiberlight

/21/ Ocean Optics, Dunedin, FL (US), "Data sheet about fiber-optic spectrometer and assemblies

/22/ M. Huebner, H. Meyer, K.-F. Klein, G. Hillrichs, M. Ruetting, M. Veidemanis, B. Spangenberg, J. Clarkin, G. Nelson: „Fiber-optic systems in the UV-region". SPIE-Proc. BiOS'00, Vol. 3911, pp. 303-312 (San Jose, Jan. 2000)

/23/ K.-F. Klein, R.Arndt, G. Hillrichs, M. Ruetting, M.Veidemanis, R.Dreiskemper, J. Clarkin, G. Nelson: „UV-fibers for applications below 200 nm". SPIE-Proc. BiOS'01, Vol. 4253, pp. 42-49 (San Jose, Jan.01)

/24/ K.-F.Klein, C.P.Gonschior, D.Beer, H.S.Eckhardt, M.Belz, J.Shannon, VK Khalilov, MB Klein, C.Jakob: "Silica-based UV-fibers for DUV applications: current status (Invited Paper)". SPIE-Proc. Vol. 8775, paper 8775-10 (Prague April 2013)

/25/ K.F.Klein,P.Schliessmann,E.Smolka,M.Belz,W.J.O.Boyle,K.T.V.Grattan: "UV-stabilized silica based fiber for application around 200 nm wavelength". Sensors and Actuators B, Vol. 38-39, pp. 305-309 (1997)

/26/ K.-F.Klein, R.Kaminski,S.Hüttel, J.Kirchhof, S.Grimm, G.Nelson: "Lifetime improvements and of UV-improved fibers for new applicatons". SPIE-Proc.Vol. 3262C (BiOS'98), pp. 150-160 (San Jose, Jan. 1998)

/27/ R.W.Lee: Diffusion coefficient of hydrogen in silica". J.Chem.Phys. Vol. 36, pp. 1062ff (1962)

/28/ J. Kirchhof, P.Kleinert, W. Radloff, E.Below: „Diffusion processes in lightguide materials". Status solidi (a), Vol, 101, pp. 391-401 (1987)

/29/ J.Stone: "Interactions of Hydrogen and Deuterium with Silica Optical Fibers: A Review". IEEE J.Lightw.Techn., Vol. LT-5, pp. 712-733 (1987)

/30/ H.Fabian,U.Grzesik,G.Hillrichs,W.Neu: "Optical fibers with enhanced performance for excimer laser power transmission at 308 nm". SPIE-Proc. Vol.1693, pp. 24-28 (Los Angeles, Jan.1993)

/31/ J.Vydra,G.Schötz: „Improved all-silica fibers for deep UV-applications". SPIE-Proc. Vol. 3596 (BiOS'99), paper 3596-25 (San Jose, Jan. 1999)

/32/ V.Kh.Khalilov, K.-F.Klein, J.Belmahdi, R.Timmerman, G. Nelson: "High-OH fibers with higher stability in the UV-region". SPIE-Proc. BiOS'06, Vol. 6083, paper 6083-08 (San Jose, USA, Jan.06)

/33/ J. Heimann, K,-F. Klein, C.P. Gonschior, M. Klein, G. Hillrichs, "Optical fibers for 355 nm pulsed lasers and high-power broadband light sources", SPIE Proc., Vol. 8576, paper 8576-19, 2013

/34/ V. Khalilov, J.Shannon, R.Timmerman: "Improved Deep UV Fiber for Medical and Spectroscopy Applications", SPIE-Proc. BiOS'15, Vol. 8938, paper 8938-9 (San Francisco, USA, Feb.14)

/35/ V. Khalilov, J.Shannon, R.Timmerman, D. Geshell: "Improved Deep UV Fiber for Medical and Spectroscopy Applications", SPIE-Proc. BiOS'15, Vol. 9317, paper 9317-14 (San Francisco, USA, Feb.15)

/36/ TransMIT GmbH, Giessen (Germany): Data sheet about certified UV-fibers (2010)

/37/ J.Assmus, J.Gombert, K.-F.Klein, G. Nelson,J.Clarkin: „Improvements in UV transmission of all-silica optical fibers with low-OH content". SPIE-Proc. BiOS 99, Vol. 3596, pp. 108-114 (San Jose, Jan. 1999)

/38/ V.Kh.Khalilov, K.-F.Klein, G.Nelson: "Low-OH all-silica fiber with broadband transparency and radiation resistance in the UV-region". SPIE-Proc. BiOS'04, Vol. 5317, paper 5317-9 (San Jose, Jan.04)

/39/ Energetiq, Woburn (USA): "Data sheets about Laser-Driven Light-Source (www.energetiq.com)

/40/ E.F.Schubert, H.W.Yao (chairmen): SPIE-Proc. 4996A "Light-Emitting Diodes:: Research, Manufacturing, and Applications" (San Jose, Jan.2003)

/41/ Nichia Corp.: Nichia Corp.: Data sheet about UV-LEDs, STSE - CC5008A

/42/ CryLas, Berlin (Germany): Brochure about low-power Nd:YAG-lasers for UV-applications

/43/ T. Tobisch, H. Ohlmeyer, H.Zimmermann, S.Prein, J.Kirchhof, S.Unger, K.-F.Klein: „ Improvement of specialty fiber damage at 266 nm wavelength", SPIE Proc., Vol. 8938, paper 8938-14, 2014

/44/ E.J.Friebele, M.E.Gingerich: "Photobleaching Effects in Optical Fiber Waveguides". Appl.Optics, Vol.20, pp.3448 (1981)

/45/ K.-F.Klein, B. Spangenberg, H.Meyer, J.Mannhardt, J.Macomber: „New analytical applications with UV-fiber bundles". SPIE-Proc. BiOS'01, Vol. 4253, pp.168-175 (San Jose, Jan.01)

/46/ K.-F. Klein, B. Spangenberg, B. Ahrenz: "Fluorescence in the fiber-optic HPTLC-method". SPIE-Proc. BiOS'02, Vol. 4616, paper 4616-30 (San Jose, Jan.02)

/47/ B.Spangenberg, K.-F.Klein, J. Mannhardt: „High Performance Thin Layer Chromatography using Fiber-Optics and Diode-Array Detection". SPIE-Proc. BiOS'02, Vol. 4625, paper 4625-24 (San Jose, Jan.02)

/48/ B.Spangenberg, C.Poole, C.Weins: Quantitative Thin-Layer Chromatography: A Practical Survey". Springer, 2011, ISBN 978-3-642-10727-6

/49/ WPI Inc. Sarasota: Data sheets about flow cells (www.wpiinc.com)

/50/ J&M Analytik AG, Essingen (Germany): Data sheets about Fiber-Optic Spectrometer (www.j-m.de)

/51/ J.Werner, M.Belz, K.-F.Klein: "UV and VIS far field intensity profile of optical fiber based flow cells", SPIE Proc., Vol. 9317, paper 9317-9, 2015

/52/ H.-S. Eckhardt, L. Lagesson-Andrasko, V. Lagesson, K.-F. Klein, K.T.V.Grattan: "Towards a fiber-optic detection device for GC-UV". Proc. of "29th international symposium on capillary chromatography" and "3rd GCxGC symposium" (Riva, Italy, May-June 2006)

/53/ L.Lagesson-Andrasko, V.Lagesson: "Handbook of ultraviolet spectra: Vapor phase 163 to 330 nm". ISBN 91-975582-1-4

/54/ H.-S. Eckhardt, K.Graubner, K.-F. Klein,T.Sun, K.T.V.Grattan: "Fiber-optic based gas sensing in the UV region" SPIE-Proc. BiOS'05, Vol. 6083, paper 6083-35 (San Jose, USA, Jan.06)

/55/ G.Marowsky,F.Lewitzka,P.Karlitschek,U.Bünting,M.Niederkrueger: "Miniaturized laser-induced fluorescence system with fiber optic probe for the analysis of acromatic compounds". SPIE-Proc.,Vol. 3539, pp- 2-9 (Boston, Nov. 1998)

/56/ P. Karlitschek, "Fiber-optic studies related to UV-laser-based sensor for pollutants (in German)," ISBN-10: 3895888281, Cuvillier publisher, Goettingen (1998)

/57/ M.Koehler, H.Dietz, Y.Maatsuura, M.Miyagi,K.-F.Klein, G.Hillrichs: Status and improvements of the UV laser scalpel", SPIE-Proc., Vol. 4717 (BiOS'97), paper 4717-12 (SanJose, February 2003)

/58/ K.F.Klein,L.S.Greek,H.G.Schulze,M.W.Blades,C.A.Haynes,R.F.B.Turner: „Fiber-guided tunable UV-laserlight system around 215 nm". SPIE-Proc., Vol. 2977 (BiOS'97), paper 2977-14 (SanJose, February 1997)

/59/ H.G.Schulze, C.J.Barbosa, L.S.Greek, R.F.B.Turner, .A.Haynes, K.-F.Klein, M.W.Blades: „Advances in fiber-optic based UV resonance Raman spectroscopy techniques for anatomical and physiological investigations". SPIE-Proc., Vol. 3608 (BiOS'99), pp.157-167 (San Jose, Jan. 1999)

/60/ H.G.Schulze,L.S.Greek,M.W.Blades,A.V.Bree,B.B.Gorzalka,K.-F.Klein,R.F.B.Turner: "Development of optical fiber sensor probes for rapid remote *in-situ* spectroscopic measurements of biological samples". SPIE-Proc. BiOS97, paper 2982-28 (San Jose, Feb. 1997)

/61/ L.S.Greek, H.G.Schulze, M.W.Blades,C.A.Haynes,R.F.B.Turner: "*In-situ* investigation of protein and DNA structure using UVRRS". SPIE-Proc. BiOS97, paper 2982-17 (San Jose, Feb. 1997)

/62/ E. Takala et al.,"Silica-Silica Polimide Buffered Optical Fiber Irradiation and Strength Experiment at Cryogenic Temperatures for 355 nm Pulsed Lasers," Cryogenics, 52, 77-81, 2011.

/63/ E.Takala: "The Laser quenching technique for studying the magneto-thermal instability in high critical current density superconduction strands for accelerator magnets". ISBN 978-951-29-5128-4, PhD-thesis, University of Turku (Finland, 2012)

/64/ J.C. Heimann, C P. Gonschior, K.-F. Klein, G. Hillrichs, E, Takala, „Spectral UV losses in 355 nm pulsed laser delivery system at low temperatures", J.Non-Cryst. Solids, Vol. 376: pp. 43-49 (2013)

/65/ M.Belz, H.-S.Eckhardt, C.P. Gonschior, G.Nelson, K.-F.Klein: "Quality control of UV resistant fibers for 200-300 nm spectroscopic applications". SPIE-Proc.Vol. 6852 (BiOS 08), paper 6852-33 (San Jose, Jan. 2008)

/66/ K.-F.Klein, M.Belz, Dress, Franke, Boyle, KTV Grattan:"Ultra-sensitive detection system for fiber optic based UV spectroscopy". SPIE-Proc. Vol. 3258 (BiOS 98), paper 3258-11 (San Jose, Jan. 1998)

/67/ Y. Matsuura, M. Miyagi ; "Aluminum-coated hollow glass fibers for ArF excimer laser light fabricated by metalorganic chemical –vapor deposition", Appl. Opt. 38, 2458 (1999)